Deep Learning on Electroluminescence Images for End-of-Line Binning of Full and Half-Cut Cells

Yoann Buratti[1], Arcot Sowmya[1], Rhett Evans[1,2,3], Thorsten Trupke[1,4] and Ziv Hameiri[1]

[1] *University of New South Wales, Sydney, Australia*
[2] *Solinno Pty Ltd, Towradgi, Australia*
[3] *5B, Alexandria, Australia*
[4] *BT Imaging, Waterloo, Australia*

End-of-line binning of solar cells ensures optimal power output of photovoltaic modules, as well as identification of misprocessed cells. Currently, binning is performed according to their electrical performance, using current-voltage (I-V) measurements. Recently, electroluminescence (EL)[1] and photoluminescence (PL)[2] imaging have been added to end-of-line inspection to improve quality control and identify defective cells. More recently, machine learning (ML) approaches with PL images of as-cut wafers have been suggested to predict end-of-line electrical parameters.[3] In this study, we propose the use of deep learning[4] and end-of-line EL imaging to replace I-V measurements as the binning method for both full and half-cut silicon solar cells.

Around 30,000 full cell EL images, together with their electrical parameters measured by an I-V tester, were collected from an R&D industrial line. The goal is to group all cells into 0.2%-wide efficiency bins, starting from a selected threshold efficiency, below which cells are binned as 'rejects'. Three subsets are randomly created from the data set: a training set 'Train' (80%), a validation set 'Val_1' (10%) and a validation set 'Val_2' (10%). A multi-step training approach is proposed. Firstly, a convolutional neural network (CNN) is trained to classify cells into the correct efficiency bin. Multiple CNN architectures are compared in this study, with five out-of-the box architectures: AlexNet,[5] ResNet,[6] DenseNet,[7] SqueezeNet[8] and VggNet;[9] and a *custom-made* architecture named EL-Net. Each network is trained independently five times on a random Train/Val_1 split (80/10) of the data set. The resulting models are then compared using two metrics: the reject recall rate, which is the fraction of correctly predicted cells of the 'reject' bin, and the cross-entropy loss (CEL).[4] The second step consists in training an ML regressor to predict the efficiency of the cell from the EL image, using the extracted features of the best performing CNN model from the first step. The focus is on the bulk of the efficiency distribution and therefore, the 'reject' bin is set aside. The output of the regressor is then binned according to the defined binning strategy of 0.2%-wide efficiency bins. In this step, multiple ML algorithms are compared: Random Forest,[10] AdaBoost,[11] Gradient Boost[12] and Neural Networks.[13] Each of the algorithms is trained five times on the training set. Then the validation set Val_2, which was set aside before step one, is used to evaluate the overall CNN+ML deep learning framework. Two scoring methods are used, the coefficient of determination (R^2) and the root mean square error (RMSE).[14]

Table I. Comparison of multiple CNN models on validation set Val_1

Model	CEL	Reject / recall rate
EL-Net	1.21 ± 0.03	0.89 ± 0.03
ResNet	1.22 ± 0.01	0.81 ± 0.07
VggNet	1.23 ± 0.02	0.78 ± 0.06
DenseNet	1.28 ± 0.02	0.68 ± 0.10
AlexNet	1.31 ± 0.01	0.83 ± 0.07
SqueezeNet	1.42 ± 0.04	0.68 ± 0.09

Table II. Comparison of ML regression models on validation set Val2

Model	R^2	RMSE
AdaBoost	0.918 ± 0.001	0.151 ± 0.001
Random Forest	0.916 ± 0.001	0.153 ± 0.001
Gradient Boost	0.906 ± 0.001	0.162 ± 0.001
Neural Network	0.774 ± 0.084	0.247 ± 0.044

As can be seen in Table I, the custom-made architecture EL-Net is one of the best performing algorithm. It has the lowest average CEL, and the highest reject recall, averaging 89%. In particular, the reject recall is significantly higher than the five out-of-the-box architectures. The best instance of the trained EL-Net achieved a CEL of 1.18 and a reject recall of 93.7%, while 98.8% of the non-reject cells

were correctly classified as non-rejects. These results highlight the potential of CNN for anomaly detection in manufacturing lines. In the second step, EL-Net is used as a feature extractor, transforming each image from the Train and Val_2 sets into a feature vector. As shown in Table II, the lowest RMSE and highest R^2 are achieved by the AdaBoost model, averaging 0.151 and 0.918, respectively. The best instance of the AdaBoost model reaches an RMSE of 0.150 and an R^2 of 0.919.

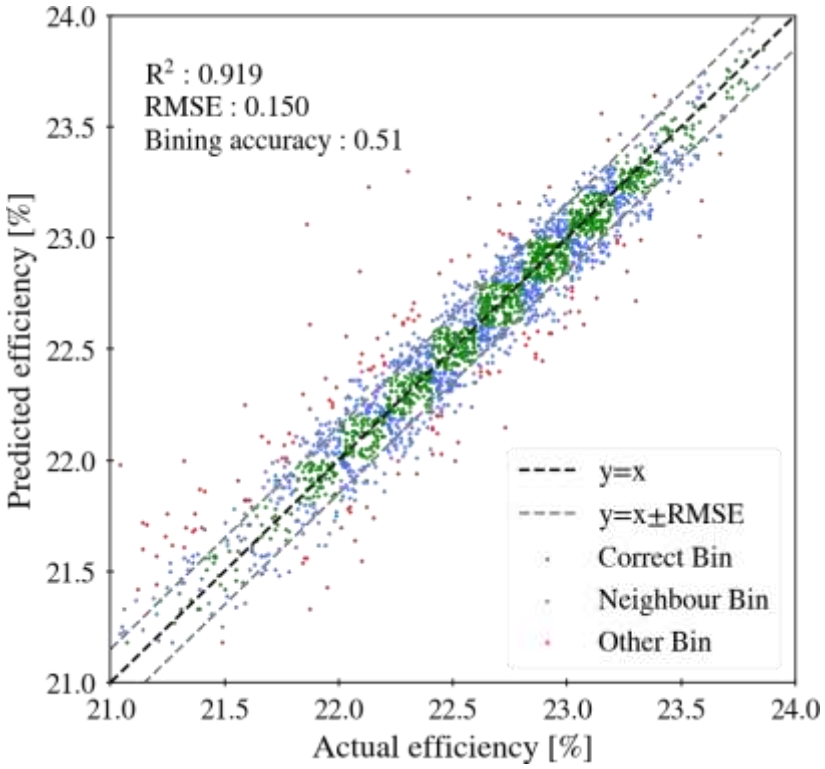

Figure 1. True vs predicted efficiency for validation set Val_2 using the best performing AdaBoost model after EL-Net feature extraction.

The measured and predicted efficiency for each cell in the Val_2 set are shown in Figure 1. The black dashed line represents the *y=x* line, while the grey dashed lines show the envelope of the prediction error within ±RMSE of the *y=x* line. 88.3% of the cells are predicted within 0.15% absolute of the actual efficiency. This indicates that the CNN+ML deep learning approach successfully predicts the cell efficiency directly from its EL image. Each cell from the Val_2 set is then binned into one of the 0.2%-wide efficiency bins: correctly binned (green), binned in a neighbouring bin (blue) or another bin (red). Binning from the regression achieves only a 51% accuracy, as it is affected by the sharpness of bin transitions. Most of the cells (95%) are predicted to be in the correct or a neighbouring bin. Evans *et al*[15] showed that in a range of ±3% relative efficiency, mismatch power loss for modules is below 0.1% for randomly sorted cells. In this study, the bin relative deviation is in average 0.7% relative, below Evan's threshold, hence, low to no mismatch power loss is expected using the CNN+ML binning.

The proposed method is now demonstrated in predicting the efficiency of half-cut cell, showing the transferability of the CNN+ML approach. The first step—training the CNN—is done on a new production dataset containing more than 30,000 cells with a smaller standard deviation of 0.3%, distinct from the Full-set (500 cells) and Half-set (1000 half-cells). The second step—ML regression of the efficiency—is performed independently on both the Full-set and the Half-set. The resulting averaged R^2 scores are shown in Table III. AdaBoost achieves a mean validation R^2 of 0.65. However, a high training R^2 suggests there is room for improvement and is likely due to the differences between full and half-cell EL images and I-V testing apparatus. Moreover, the *best* performing AdaBoost regressor achieved an R^2 on the half cells validation set of 0.74, demonstrating the potential of using deep learning analysis of EL images for sorting half-cut cells. Post-cutting binning, using a CNN+ML approach, opens exciting

possibilities of more controlled and reliable PV module manufacturing and these results are the first step into deep learning-based applications for sorting of other advanced structures. The developed approach can be easily applied to busbar less and shingles solar cells.

Table III. Comparison of ML efficiency regression models on Full and Half-cut cells

Model	Full-set Train R^2	Full-set Val R^2	Half-set Train R^2	Half-set Val R^2
AdaBoost	0.998	0.985	0.973	0.647
Random Forest	0.997	0.982	0.835	0.506
Gradient Boost	0.997	0.983	0.968	0.326

In this study, we have demonstrated a proof of concept for end-of-line efficiency binning using a deep learning framework. A custom-made algorithm (EL-Net) is trained to extract features and detect misprocessed and defective cells with 93.7% reject recall rate. The extracted features are then processed by an AdaBoost model to predict the expected efficiency of the cell, achieving a RMSE of 0.15. Finally, the CNN+ML approach is applied into predicting the efficiency of half-cut solar cells from EL images setting the stage for further applications of deep learning and luminescence imaging in post-cutting binning. Although a higher volume and variety of cell types are required, the preliminary results discussed in this work demonstrate that EL imaging on fully processed solar cells, when combined with customised deep learning approaches, can provide strong correlations with the electrical parameters that are currently gained from illuminated I-V testing. Our study suggests that ultimately the proposed EL-based (and in the future, PL-based) approach has the potential to replace illuminated I-V measurements as standard end-of-line binning tools. Furthermore, the ease of EL and PL imaging on half-cut or shingled cells, makes it a promising technique for binning and filtering out of defective cells after the cutting process.

References

1. Fuyuki, T., Kondo, H., Yamazaki, T., Takahashi, Y. & Uraoka, Y. Photographic surveying of minority carrier diffusion length in polycrystalline silicon solar cells by electroluminescence. *Appl. Phys. Lett.* **86**, 262108 (2005).
2. Trupke, T., Bardos, R. A., Schubert, M. C. & Warta, W. Photoluminescence imaging of silicon wafers. *Appl. Phys. Lett.* **89**, 044107 (2006).
3. Demant, M., Virtue, P., Kovvali, A. S., Yu, S. X. & Rein, S. Deep learning approach to inline quality rating and mapping of multi-crystalline Si-wafers. in 5 (2018).
4. Goodfellow, I., Bengio, Y. & Courville, A. *Deep learning*. (MIT press, 2016).
5. Krizhevsky, A., Sutskever, I. & Hinton, G. E. ImageNet classification with deep convolutional neural networks. *Adv. Neural Inf. Process. Syst. 25* 1097–1105 (2012).
6. He, K., Zhang, X., Ren, S. & Sun, J. Deep residual learning for image recognition. *ArXiv151203385 Cs* (2015).
7. Huang, G., Liu, Z., van der Maaten, L. & Weinberger, K. Q. Densely connected convolutional networks. *ArXiv160806993 Cs* (2018).
8. Iandola, F. N. *et al.* SqueezeNet: AlexNet-level accuracy with 50x fewer parameters and <0.5MB model size. *ArXiv160207360 Cs* (2016).
9. Simonyan, K. & Zisserman, A. Very deep convolutional networks for large-scake image recognition. 14 (2015).
10. Breiman, L. Random forests. *Mach. Learn.* **45**, 5–32 (2001).
11. Drucker, H. Improving regressors using boosting techniques. in *ICML* (1997).
12. Friedman, J. H. Stochastic gradient boosting. *Comput. Stat. Data Anal.* **38**, 367–378 (2002).
13. Hinton, G. E. Connectionist learning procedures. *Artif. Intell.* **40**, 185–234 (1989).
14. Glantz, S. A. & Slinker, B. K. *Primer of applied regression and analysis of variance*. (New York (N.Y.) : McGraw-Hill, 1990).
15. Evans, R. & Boreland, M. Multivariate data analytics in PV manufacturing—four case studies using manufacturing datasets. *IEEE J. Photovolt.* **8**, 38–47 (2018).